An Analysis of Zambian Cast-Aluminum Pots

Pinar Demetci, Michael Resnick, Mariko Thorbecke, and Anne Wilkinson
Olin College of Engineering
Needham, Massachusetts 02492

***Abstract*—Aluminum pots cast by Zambian small business owners often fail under normal use scenarios. This is due to the brittle nature of contaminants introduced by recasting scavenged alluminum-silicon alloys. If the brittleness of the Al-Si alloy is due to large grain size, nucleating agents such as sodium may be used to refine the grain and provide increased toughness. Recasting the Zambian pots with small additions of table salt (NaCl) did lead to a small average increase in ultimate tensile strength and toughness across three trials, but the samples were still brittle and failed easily. This led to an investigation of fracture surfaces and failure modes. The castings are shown to fail along acicular regions of an iron-rich contaminant. These contaminants provide easy crack propagation paths and overwhelm the benefits of nucleating agents. Future work would involve researching methods of either using a morphological agent to change the shape of the acicular regions or removing contaminants from the aluminum alloys added into the castings.**

***Keywords*—Casting, Aluminum-Silicon Alloy, Zambian Pots, Grain Refinement**

I. Introduction

Cast aluminum pots made from recycled metal are commonly used for cooking in Zambia. The pots are sand cast by small business owners that scavenge for scrap metal. The scrap metal is melted down in furnaces and recast into pots Figure 1. Due to the random composition of the scavenged metal and potential iron contamination from the casting crucible, the resulting alloy is brittle and these pots often structurally fail during normal use, such as being pushed along a table surface or dropped from a small height.

Fig. 1. Casting process in Zambia. Scavenged scrap aluminum is melted down in an iron crucible and stirred with an iron rod. The molten alloy is then poured into sand molds to form pots.

In spring of 2014, a student team at Olin College researched a variety of approaches to reduce brittleness and increase strength in the aluminum alloy castings. This team researched a variety of measures that could be taken to improve the strength of these pots. A measure that showed promise was adding NaCl to the alloy.

Adding the appropriate nucleating agent can reduce eutectic grain size. A finer grain structure is desirable because it leads to improved mechanical properties, such as higher ultimate strength, and improved toughness [1]. The aforementioned failure analysis team ran experiments involving two nucleating agents, sodium and strontium, and found that sodium addition resulted in the greatest increases in energy absorption. NaCl is a great candidate for use in the Zambian casting process because, unlike strontium, it is readily available in Zambia and cheap.

This study tested the hypothesis put forth by previous research that recasting a sample of a cast conglomerate of recycled aluminum-silicon alloys, adding 0.03% sodium by weight would decrease brittleness due to the salt acting as a nucleating agent for aluminum. Samples were chosen from two different pots to demonstrate efficacy over a range of compositions. Both tensile and impact tests were performed to observe changes in overall strength as well as energy absorption since the pots being studied typically fail under dynamic loading.

II. Alloy Composition

In order to determine the range of compositions present in a typical cast aluminum pot and lid, five different samples were sent out for optical emission spectroscopy analysis (see "Acknowledgements"). The compositional breakdown of each sample is given in Table I. Alongside this data are the recommended ranges for various common contaminants of the UNS A03320 alloy, which was found to be most chemically similar to the alloys studied here. For comparison, a bar graph of each element (excluding Aluminum) is shown in Figure 2.

	Z0	Z1	Z2	Z3	Z4	UNS A03320
Aluminum	83.30%	85.70%	87.30%	83.40%	86.30%	remainder
Silicon	8.60%	9.90%	9.90%	8.00%	6.70%	10.5%
Copper	2.00%	2.40%	2.30%	1.90%	3.20%	2.0-4.0%
Zinc	0.70%	2.10%	2.10%	2.00%	1.80%	1.0% max
Iron	0.70%	1.20%	1.30%	1.10%	1.30%	1.2% max
Nickel	0.10%	0.50%	0.50%	0.20%	0.50%	0.5% max
Magnesium	0.30%	0.00%	0.00%	0.00%	0.30%	0.5-1.5%
Manganese	0.20%	0.20%	0.20%	0.10%	0.10%	0.5% max
Other	0.20%	0.40%	0.30%	0.30%	0.40%	0.5% max

TABLE I. Pot compositions

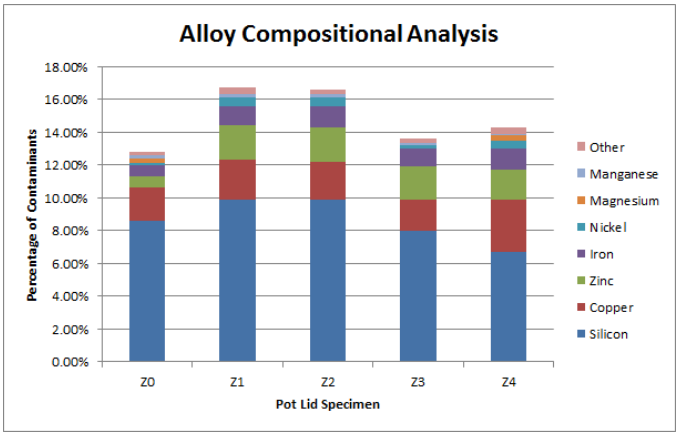

Fig. 2. Percentage of the other elements present in the five cast aluminum alloy samples.

Fig. 3. The two pot lids chosen for experimentation. Z4 (left) and Z1 (right).

The pots clearly exhibit a wide range of compositions, which is consistent with the unpredictability of their strength and ductility. Because of the variety of scraps used in this pot casting process, there are far more contaminants present than there are in typical Al-Si alloys, which usually ideally have 2-4 alloying elements. Although several of these elements, such as silicon and copper, can improve strength and others, such as manganese, typically have a neutral effect on mechanical properties, some contaminants, iron in particular, are widely known to increase brittleness significantly, even when in trace quantities. Additionally, although many aluminum alloys use silicon percentages much higher, even 0.01 wt% silicon is enough to substantially impact mechanical properties by dissolving in the alpha-solid solution and helping prevent dislocation motion by producing irregularities in the lattice [8].

> "Liquid aluminium is capable of dissolving iron from unprotected steel tools and/or furnace equipment. Equilibrium Fe levels can reach 2.5 wt% in the liquid phase at normal melt temperatures of 700°C and up to 5 wt% for a melt held at 800°C" [7].

Thus it may be useful to note that when using an iron-based crucible, like the one used to produce the pots being studied, using a lower melt temperature will result in less iron introduction. It is likely, however, that the melt temperature is kept as low as possible anyway to save energy.

III. Experimental Methods

The efficacy of any recommendation made for toughening an alloy will vary depending on composition. Because of the random composition, any recommendation made for strengthening the alloy must apply to a wide range of alloys. Of five Zambian-cast pot lids, labeled "Z0" through "Z4", the two that were the most distinct from each other in terms of grain size, color, and surface finish were chosen for experimentation. These lids were labeled as "Z1" and "Z4", the former being lighter colored and shinier, with visibly larger grains.

In order to compare the mechanical properties before and after addition of a nucleation agent, a .03% wt fraction of NaCl was added to half of the samples, the value recommended in the ASM handbook [4].

A total of 12 impact test specimens and 12 tensile strength test specimens were cast using investment molding. Specimen geometry and dimensions are shown in figure 4 The salt was added to the aluminum before melting and then stirred when the aluminum melted. Boric acid powder was added to the melt in order to prevent oxidation. Prior to testing, samples were cleaned of flash and other surface imperfections from the casting process.

Impact and tensile strength tests were run on samples from both lids, cast both with and without salt. The tests were run with three specimens for each case. An Instron Impact Tester was used to apply a dynamic load of 25.9 joules to the impact samples. The samples were oriented so that the notched side would face down. The tensile strength tests were conducted on the Instron single column universal testing system using a 5000 kN load cell.

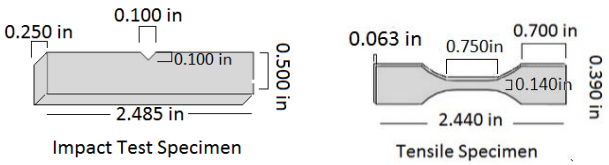

Fig. 4. Cast specimens used for mechanical testing. The impact specimen has dimensions 2.49" x 0.5" x 0.25", with notch depth and width of 0.10". The tensile specimen has major dimensions of 2.44" x 0.39" x 0.063".

Microstructural analysis was performed on polished samples of Z1 and Z4, as well as on the fracture surfaces. EDS was performed on the fracture surfaces in order to identify the chemical composition of each region.

IV. Microstructural Analysis

Microstrucutral analysis was performed on both NaCl modified and unmodified samples of the pot recastings. Long, acicular regions and rosette regions in particular were identified as phases containing contaminants. In addition, microstructures

showed substantial differences in composition between Z1 and Z4. For example, in pot lid Z1, the micrograph without salt (Figure 5) contains no dendrites. This suggests that the entire sample is a eutectic solid with large grain size, where large light grey regions correspond to the aluminum-rich alpha solid, and the dark grey region is a silicon beta solid. The irregular regions are a smaller eutectic grain caused by faster cooling within the localized area. Comparison to the ASM handbook micrographs suggested the light grey acicular regions were an iron-rich intermetallic compound. There are three possible candidates for the composition of the contaminant: $Fe_2Si_2Al_9$, Cu_2FeAl_7, and Fe_3SiAl_2. After close examination of the different microstructures formed by these solids, the $Fe_2Si_2Al_9$ solid bore the most resemblance to the acicular spikes seen [5]. Without salt, the solid aluminum regions that formed were relatively smaller and disjointed. When salt was added, (Figure 6) it appeared to increase the grain size of the eutectic aluminum solid. In addition, large iron spikes are present in both castings, and the salt appears to have made those acicular regions larger.

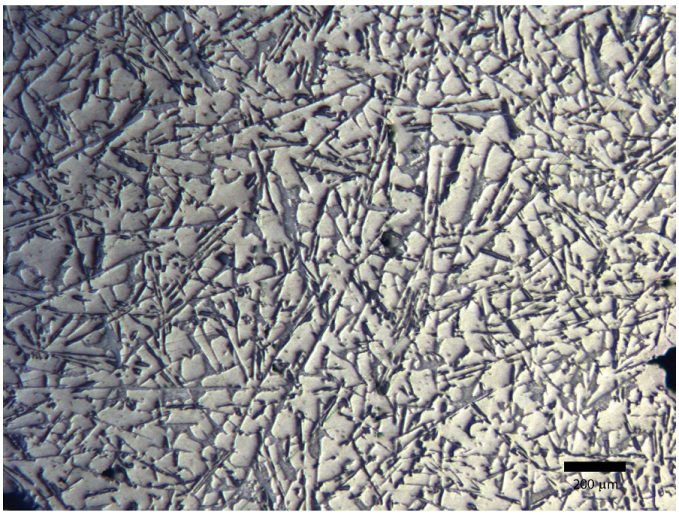

Fig. 5. Z1 without salt modification. Light grey regions are aluminum rich alpha solid, and dark grey regions are silicon beta solids. Long light grey acicular spikes are an iron-containing intermetallic impurities. The lack of alpha dendrites suggest a eutectic composition for Z1.

Z4 has a smaller overall grain size than Z1, and appears to be hypo-eutectic (Figures 7 and 8). This explains the large percentage of aluminum-rich alpha solid. The alpha solid, consistent with many aluminum alloys, formed a long, rounded dendritic structure resembling a backbone. This structure is present especially in the modified sample. In Z1, the salt resulted in a more rounded alpha solid. The iron-rich acicular regions became sparser and larger in all modified samples. The reason hypothesized is that the salt acts as a nucleating agent for the iron-based intermetallic, allowing it to form earlier and have more time to create large regions. It could also be because larger alpha dendrites forming in the modified samples could have pushed iron contaminant phases together.

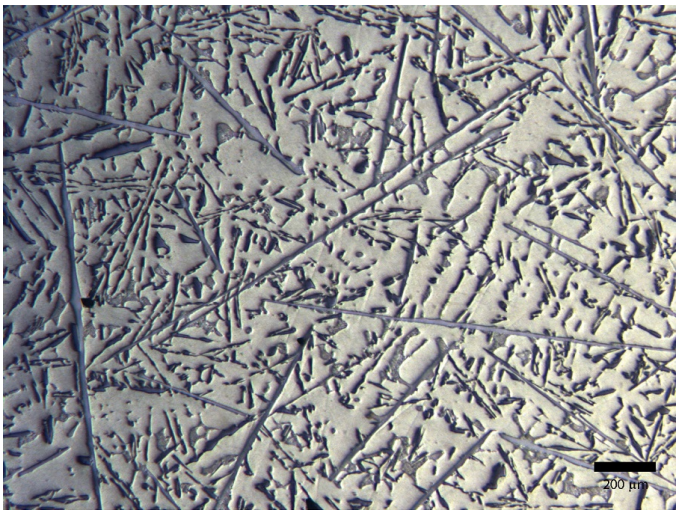

Fig. 6. Z1 with salt modification. The alpha solids became rounder at their edges. The acicular iron regions are sparser and larger in the modified Z1 sample than the original Z1 sample.

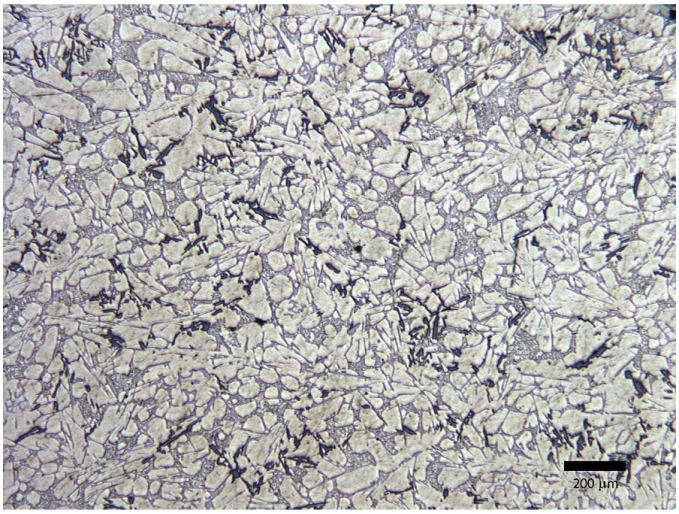

Fig. 7. Z4 without salt modification. Z4 has a much smaller grain size than Z1, and has a large concentration of alpha solid. This suggests that it is hypo-eutectic.

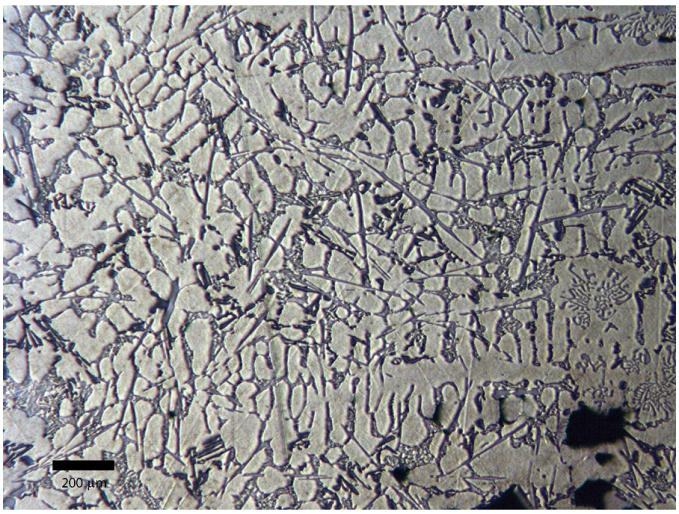

Fig. 8. Z4 with salt modification. In this sample the alpha solid formed a large dendrite structure. The iron cotaminant condensed into fewer and larger spikes than in the unmodified sample.

In addition to acicular regions of contaminants, an interesting contaminant shape present in both samples was the rosette, shown in 9. Given its shape and the fractography that follows, it appears to be a less damaging contaminant than the sharp acicular regions, and is suspected to be fairly inocuous. The rosette is likely where a lot of the copper, nickel and zinc contaminants are manifesting. The microstructure of the "rosette" most resembles that of Cu_3NiAl_6.

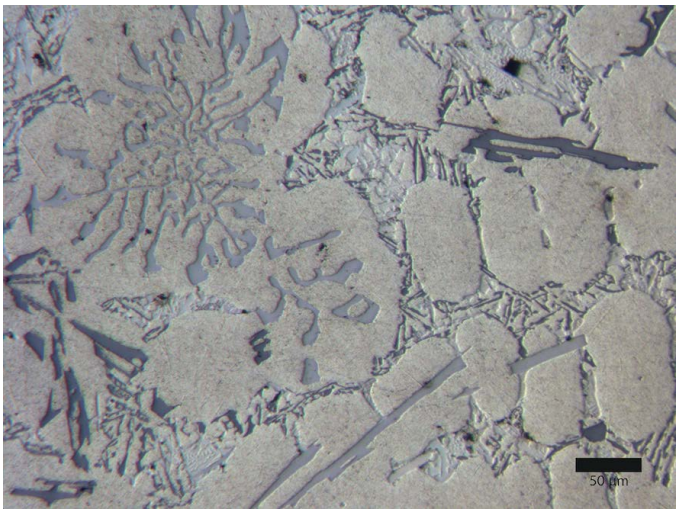

Fig. 9. The medium-grey, symmetrical region is an intermetallic impurity referred to as a "rosette". This particluar rosette is from a micrograph of a modified Z4 sample, but is present in all of the samples.

V. Fractography

Fracture surface images of the impact specimens were captured using stereo microscopy, optical microscopy, and scanning electron microscopy (SEM) in order to identify the areas of brittle fracture.

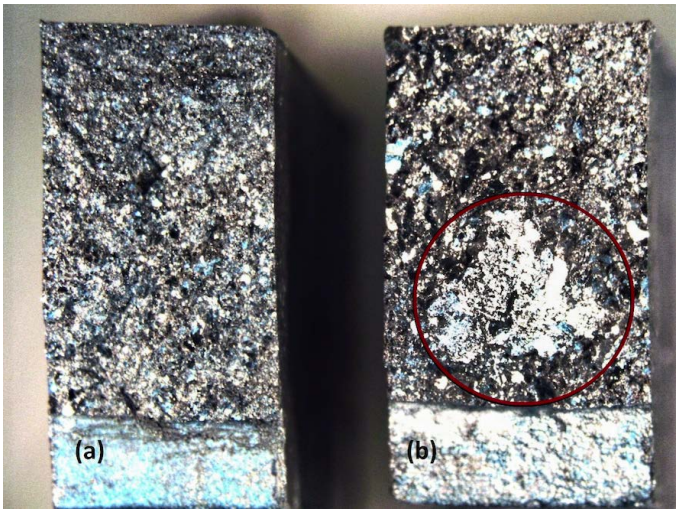

Fig. 10. Stereo microscopy images of fracture furfaces of Z4(a) and Z1(b) after the impact testing. Z4 has more fibrous surface, whereas Z1 has more flat areas. The shiny circled region indicates that Z1 is more brittle than Z4.

Figure 10 is a macro comparison of two fracture surfaces from unmodified samples of Z1 and Z4. The major difference is that Z4 has a more fibrous surface, whereas Z1 has a more planar surface. Brittle fractures are characterized by cracks running perpendicular to the applied stress. [3] These perpendicular fractures create flat surfaces. The bright region of the Z1 surface circled in Figure 10 is an example of flat surfaces indicative of brittle fractures. By contrast, ductile fracture surfaces are rougher in appearance due to the plastic deformation the material undergoes. [3]

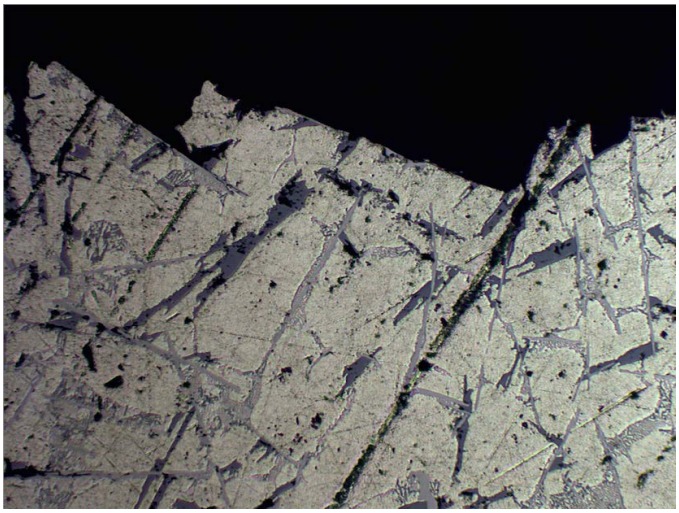

Fig. 11. Optical microscopy image of fracture surface on Z1. The crack follows the gray-colored acicular structures that are identified as iron-rich regions in EDS.

Brittle fractures can either follow a transgranular or an intergranular path. [3] In transgranular fractures, the crack passes through the grains and changes directions from grain to grain due to different lattice orientation of atoms in the grain. In intergranular fractures, the crack travels along the grain boundaries, especially when the phase in the grain boundary is brittle. [3] A micrograph of the Z1 fracture surface is shown in

Figure 11. Cracks followed the structures that were identified as gray-colored iron-rich acicular regions. This confirms that the brittle fracture followed an intergranular path.

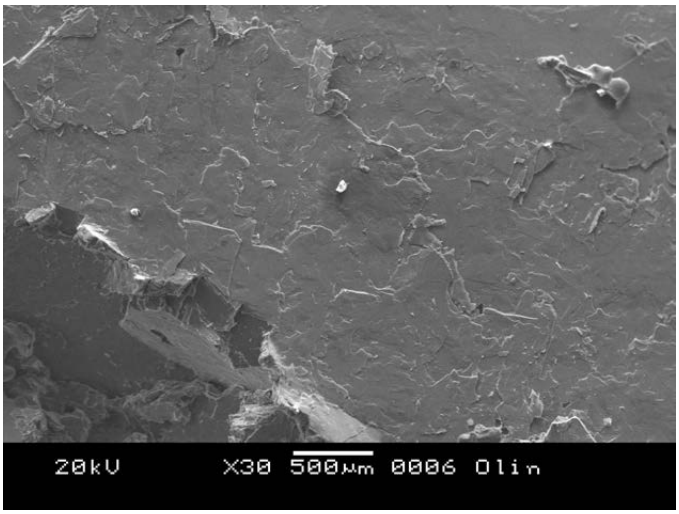

Fig. 12. SEM image of the large planar region of Z1 that was circled in Figure 10. EDS analysis confirmed that these were iron-rich regions.

An SEM image of the circled flat area from Figure 10 is given in Figure 12. Using EDS, this flat region was identified as an iron-rich region. This implies that the acicular needle-like structures in the optical microscopy images are in fact iron-rich plates. Additional SEM images of Z1 and Z4 are displayed in Figures 14 and 13, respectively. Z1 has more iron-rich plates, whereas Z4 has more dendrites (circled in Figure 13). The dendrites were identified as the aluminum-rich ductile regions of the alloy in the "Microstructure" section. This is consistent with the compositions found through EDS analysis. (see "Energy Dispersive X-Ray Spectroscopy(EDS)" section). The Z4 alloy likely has more dendrites due to the higher percentage of aluminum. The difference between the number of dendrites and iron plates in Z1 and Z4 might be the primary reason why one is more brittle than the other. In general, ductile fractures are more desirable because the plastic deformation leads to slower crack propagation and more total energy absorbed before failure.

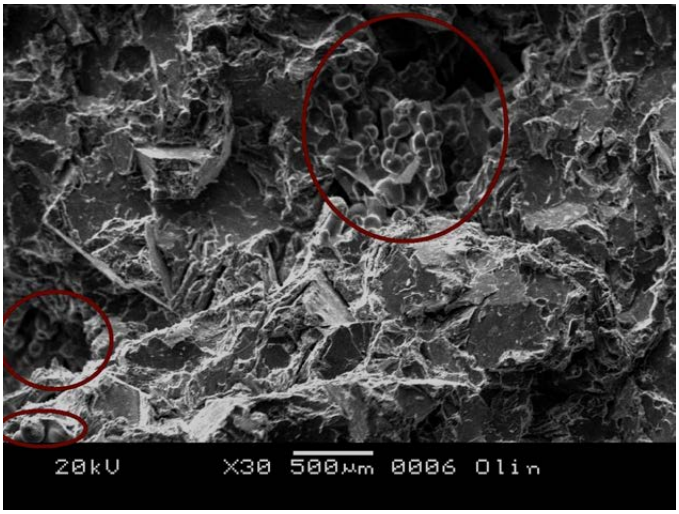

Fig. 13. SEM image of fracture surface of Z4. Circled areas show aluminum-rich dendrites that are more ductile structures in the alloy.

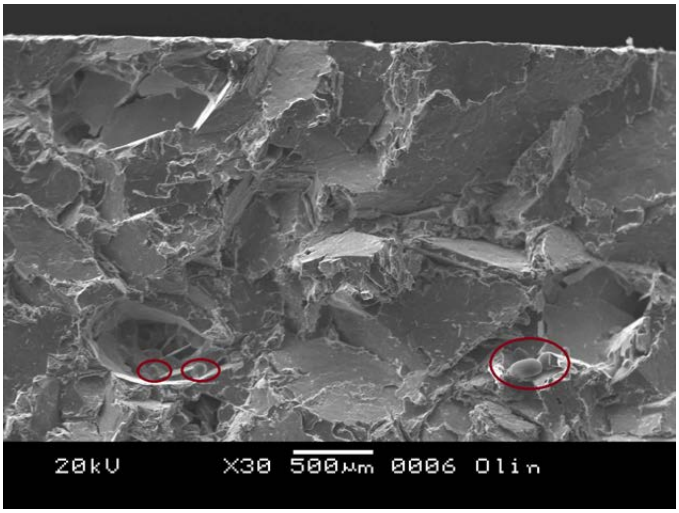

Fig. 14. SEM image of the fracture surface of Z1. Circled areas show aluminum-rich dendrites. Note that there are more aluminum-rich dendrites in the SEM images of Z4, whereas there are more iron-rich flat areas in Z1. This suggests that the primary reason why Z1 went through a brittle fracture is due to having less dendrites and more large iron-rich plates in its microstructure. In fact, the compositional analysis of Z4 resulted in more aluminum percentage than Z1 (86.30% and 85.70%, respectively).

VI. Energy Dispersive X-Ray Spectroscopy(EDS)

A. *Spot Analysis*

From the fractography, it is clear that the alloy is undergoing brittle fractures along the flat planes of the fracture surface, and the acicular regions of the microstructure. Through microstructural analysis and comparing the acicular regions to impurities commonly found in aluminum alloys, $Fe_2Si_2Al_9$ was identified as the most likely candidate. EDS spot analysis was performed on one of the flat surfaces of the fracture surface in order to confirm the identity of the acicular impurity. Figure 15 is an image of an impact specimen from Z4, with six different points used for EDS analysis. The chart in Figure 16 corresponds to the energy profiles of the compounds contained

in point 3, which is located on the flat surface of a brittle fracture.

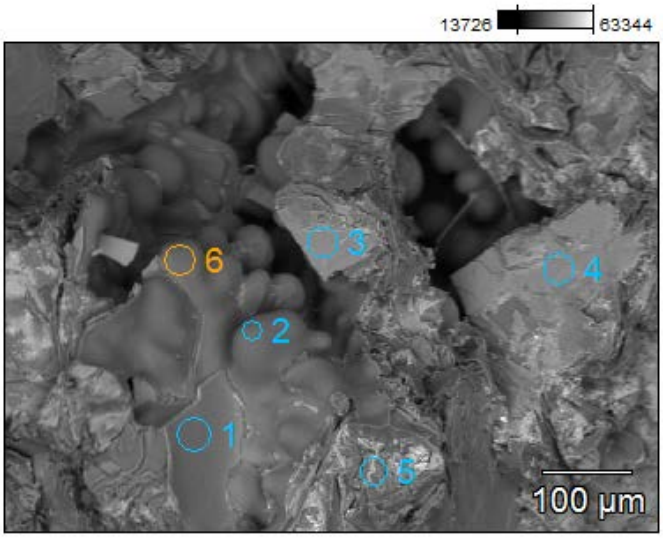

Fig. 15. Fracture Surface of Z4, with six different points sampled for EDS analysis. The energy profile charts for points 3, 6, and 5 respectively are present in figures 16, 17, and 18.

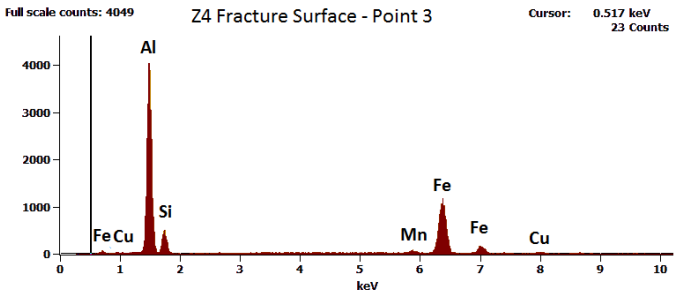

Fig. 16. Chemical Composition of Point 3. Point 3 was sampled from a flat surface region. The large amount of iron supports the hypothesis that the alloy is fracturing along iron impurities.

The large percentage of Al, Fe, and Si confirms $Fe_2Si_2Al_9$ as the acicular impurity and brittle plane. In addition to the brittle fracture surfaces, the round dendritic protrusions were also analyzed in order to confirm their identity as aluminum alpha solid. Point 6 of Figure 15 is positioned on one of the dendrites, and its corresponding energy profile chart is shown in Figure 17.

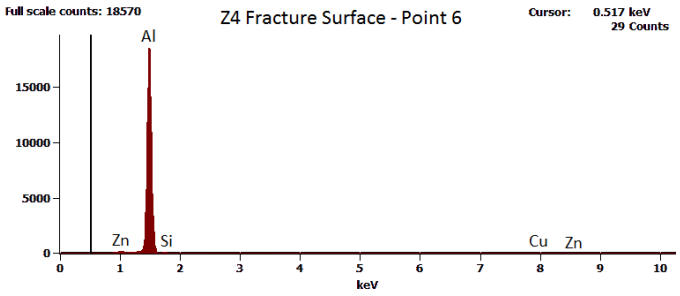

Fig. 17. Chemical Composition of Point 6. Point 6 was positioned directly over an alpha solid dendrite. This explains the almost pure Aluminum composition.

The dendrites were confirmed to be nearly pure aluminum. Finally, in this sample of Z4, point 5 (Figure 15 was hypothesized to be a region of aluminum-silicon eutectic.

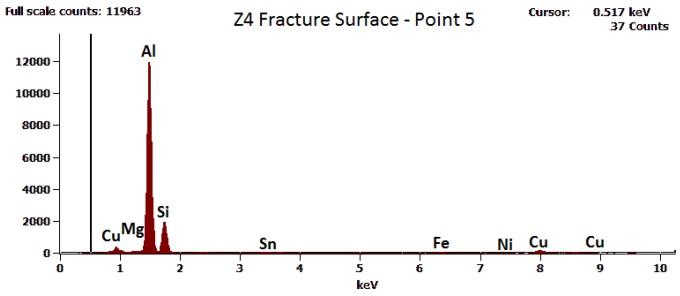

Fig. 18. Chemical Composition of Point 5. Point five was positioned over a mottled, irregular region of the fracture surface. The large amount of aluminum and smaller amount of Silicon suggest that this is part of the Al-Si eutectic.

Point 5 (Figure 15) does appear to have appropriate amounts of Al and Si to be classified as eutectic (12.2% Si, 82.8% Al). The Z1 fracture surface (Figure 19 had many of the same characteristics as the Z4 fracture surface. Points sampled from flat surfaces had a high concentration of iron, and more ductile fracture surfaces had higher concentrations of aluminum. A medium grey, symmetrical impurity described in the microstructure section as a “rosette” is present in Figure 19. Its composition is analyzed in the energy profile chart for point 3 in Figure 20.

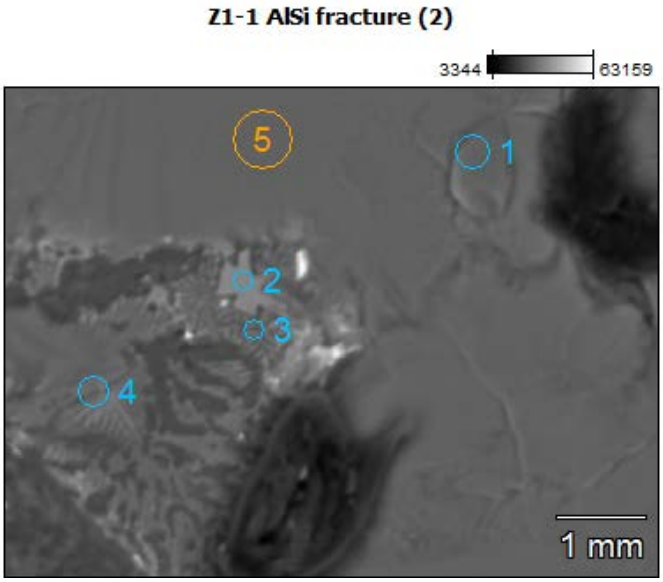

Fig. 19. Fracture surface of Z1, with five different points sampled for EDS analysis. The energy chart for point 3 is given in Figure 20

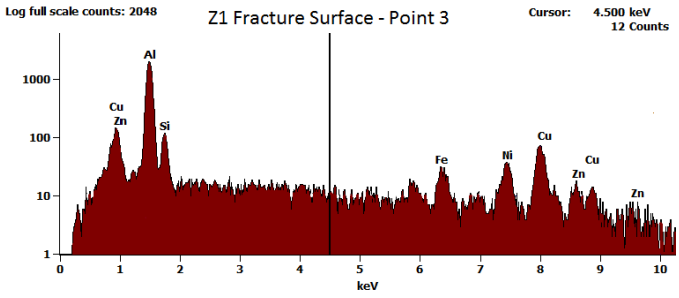

Fig. 20. Chemical Compostion of Point 3. Point 3 was sampled from a symmetrical, light-grey "rosette" region of impurities. The results display a large number of very different compounds. The rosettes are likely where many of the Cu, Ni, and Zn impurities are manifesting.

The "rosette" has a large mix of different contaminants. By examining microstructures, Cu_3NiAl_6 was hypothesized to be the primary component. There is certainly copper, aluminum, and nickel present in this area but there are some other elements such as zinc or iron which are unaccounted for.

VII. Mechanical Property Analysis

The objective of adding salt to the castings was offer the alpha solid extra nucleation sites so that more solids of smaller size would form. The grain-refining process generally helps to increase the energy needed for crack propagation, and so it is expected to increase toughness and strength.

A. Impact Testing

The bars on Figure 21 display the average energy absorption for each set of tests. The results show that original Z4 samples absorbed 48.27% more energy than original Z1 samples on average (0.76 J and 0.51 J, respectively). Overall, the Z4 samples were less brittle and took more time to fracture, leading to higher energy absorptions. The optical microscopy images for Z4 show larger primary aluminum dendrites compared to Z1. These dendrites are soft and ductile. Thus, they help absorb more energy via plastic flow. Additionally, the large number of acicular iron-rich contaminants in Z1 provide an easy path for crack propagation without any dislocation motion. Finally, Z4 samples had finer eutectic grains than Z1. Finer grains require a propagating crack to change directions more frequently, resulting in more energy needed to continue propagation.

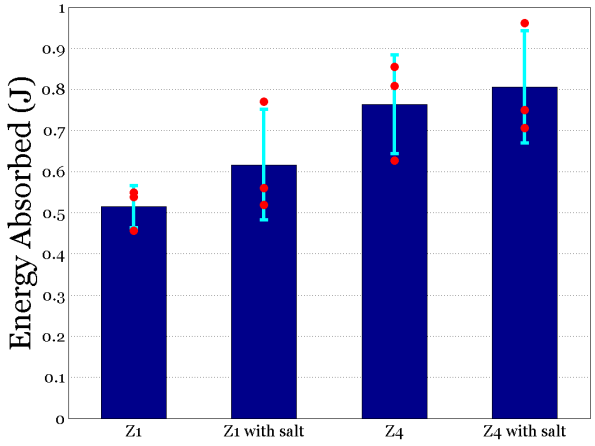

Fig. 21. Energy absorption during impact with standard deviation bars. Overall, Z4 performed better than Z1. There was also a marginal increase in energy absorption in the modified samples.

NaCl addition increased energy absorption throughout impact on average. Z1 samples with NaCl addition absorbed 19.82% more energy than Z1 original samples did on average (0.62 J and 0.51 J, respectively). Z4 samples with NaCl addition absorbed 5.58% more energy than Z4 original samples on average as well (0.81 J and 0.76 J, respectively). The smooth dendritic alpha regions present in the NaCl samples lends a more ductile structure. However, the iron-rich acicular phases are also fewer and longer in the NaCl samples, allowing for easier crack propagation. This has the potential to overwhelm the potential benefits of the ductile alpha dendrites since most fracture surfaces would be most likely to occur along the iron spikes.

The mean of energy absorption results suggest an increase in the impact toughness of the alloy with the addition of NaCl. However, the large overlap between the standard deviation bars demonstrate the variation between results for each individual sample. In order to validate the effect of NaCl addition on impact toughness, more tests would need to be run with a larger sample size.

B. Tensile Strength

Increases in average tensile strength were seen after addition of NaCl in both Z1 and Z4 (22). The variance in strength values add an element of randomness to our tests, and as a result it is difficult to make a strong conclusion about the effect of salt addition on tensile strength. The confidence interval for the modified Z4 trials, however, has no overlap with that of the Z4 original trials, providing evidence that salt addition

may increase the ultimate tensile strength of the Z4 sample on average. It is suspected that the same would be true of Z1 given the corroborating impact data, and that the large variance in measured strength is a consequence of its relatively high brittleness.

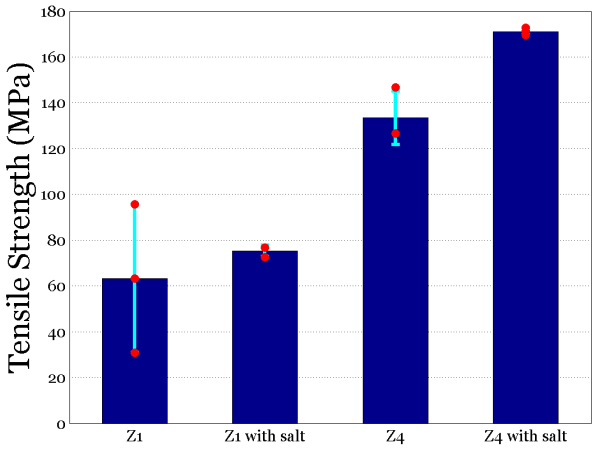

Fig. 22. Tensile yield strength. Once more, Z4 performed much better than Z1. There was also a marginal increase in yield strength with the addition of salt.

An interesting result was that the data from the modified samples had lower variance compared to the un-modified samples. Thus, adding salt to the melt could result in a more reliable product for Zambian pot casters.

Original Z4 was observed to have higher strength than original Z1, which was expected since it has larger alpha dendrite structures and a finer eutectic region. Z1's strength increase with salt addition may be due to the presence of more rounded alpha regions, which could serve to reduce stress concentrations. Z4's strength increase with salt addition may also be due to larger alpha dendrite structures than were present in the original Z4 sample.

Despite the mechanical property advantages described that resulted from salt addition, however, the iron-rich acicular regions are larger, which should provide for easier crack propagation. At this time, there is no complete explanation for the potential toughness and strength increases of these alloys with salt addition due to the increased size of the acicular regions. It is unclear as to whether adding salt would be helpful for every pot composition, as it is expected that in some cases the acicular regions would grow large enough to overwhelm the potential benefits of salt addition.

C. Sources of Error

1) Casting: During casting, melting time in the induction furnace was consistent for the majority of samples, however, there were small variations in heating times between some castings. This could affect temperature, and, consequently, cooling time, which could impact grain sizes; cooling rate increases result in less time for grain nucleation, and thus larger grains. Because we waited 8 minutes after casting to quench, however, we expect this error to be minimal. The time spent and thus efficacy of mixing the molten aluminum with salt was also likely variable.

2) Tensile testing: The jaws holding the tensile specimens were, unfortunately, not completely planar with one another, resulting in a few degrees of torsion when clamping samples. As the weaker specimens would have been more affected by this prestressing, it is possible that larger strength differences between stronger and weaker specimens were reported than there actually were as well as more variance among brittle samples was reported than there actually was.

3) Impact testing: The standard deviation bars for the impact testing results were overall larger than the ones in tensile strength testing results. One reason for such deviation might be the uncertainity with positioning the samples. The notches in the impact testing samples assisted the fracturing, however, they needed to be centered in the test set-up so that the notches would line up with the impact fixture. There might have been random parallax error if the positioning were slightly off. Additionally, some specimens' notches exhibited observable differences from others, such as shallower notch valleys and notch valleys with bumps, which could create stress concentrations. Repeating the test with a larger sample size would also help increase the accuracy.

VIII. Conclusion

Based on the results of the compositional analysis, it was clear that all five original pot samples (Z0-Z4) had very different chemical compositions. Mechanical testing was done on two of the five pots (Z1 and Z4) and this difference in composition had a major impact in test performance. Tensile strength and impact tests showed that Z4 performed better overall than Z1. In impact testing, Z4 original samples absorbed 48% more energy than Z1 original samples on average. Z4 samples also had twice as much ultimate tensile strength than Z1 on average. This may have been due to the increased alpha volume of solid in Z4 over Z1.

Addition of NaCl to both samples increased the energy absorption, indicating a decrease in brittleness. Tensile strength on average was also improved by the addition of NaCl. Z4 and Z1 samples absorbed 20% and 6% more energy, respectively, with the addition of salt. They also had respectively 19% and 28% higher tensile strength measurements when NaCl was added. However due to variation between the results of individual samples, more testing will need to be done to improve confidence in these results.

Impurities in the alloys were found to be a big issue. They provide an easy path for cracks to propagate. Even though the addition of salt appeared to enlarge the aluminum-rich dendrites, contaminants contributed to decreased performance in both samples. EDS analysis showed that rounded dendritic regions were almost pure aluminum, that flat regions were iron-rich, and that the rosette formations were a combination of copper and nickel, although the copper and nickel impurities were not believed to be major causes of the alloys' brittleness after examining the samples' fractography.

The inconsistency in composition of the pots makes it difficult to make predictions regarding how salt addition will affect brittleness of a cast pot. While the addition of sodium

enlarged the aluminum-rich dendrites, the contaminants played a big role in negating these effects. Even with the increases in strength, however, Z1 only increased from 63 to 75 MPa and Z4 from 133 to 171 MPa. Given that these are cast aluminum-silicon alloys, the expected value ranges from 131 MPa to 248 MPa, putting even the strongest of the alloys tested on the weaker end of the spectrum [6]. Eliminating contaminants, which result in high brittleness, or their detriments may be more effective than attempting to modify the alpha grain size. As such, casters should be more informed about the materials they are melting, as even trace amounts of iron can be devastating for the mechanical properties of cast aluminum-silicon alloys. Thus, if possible, the crucible used and ladle used for pouring should be coated, perhaps in a clay, since they are made of steel. Ideally, these items would not be iron-based.

It is recommended that alloys with low silicon content are chosen for the Zambian casting process to decrease brittleness. Such alloys can be found in "... applications where good casting characteristics, good weldability, pressure tightness, and moderate strength are required," such as "Ornamental grills, reflectors, general-purpose castings, automotive cylinder heads, internal combustion engine crankcases, piano plates, aircraft supercharger covers, fuel-pump bodies, air-compressor pistons, liquid-cooled cylinder heads, liquid-cooled aircraft engine crankcases, water jackets, and blower housings." Copper and zinc addition may decrease ductility, depending on the alloy, so copper or brass should not be added into the casting if possible. Also to reduce brittleness of the casting, alloys used in "automotive and diesel pistons, pulleys, sheaves, and other applications where good high-temperature strength, low coefficient of thermal expansion, and good resistance to wear are required" typically have higher silicon content, and should therefore be avoided. Furthermore, these alloys may also contain nickel, whose presence can decrease ductility and resistance to corrosion in many alloys of lower silicon content [11] p. 152–177.

IX. Future Work

"Additions of Mn, Cr, Cu, V, Mo, and W [act as morphological agents,] promot[ing] a body-centred cubic structure..." in Al-Si alloys instead of the platelet/acicular structure that is typical of Al-Si-Fe alloys [10]. In Aluminum: Properties and Physical Metallurgy, adding a 0.5% weight fraction of Mn to an Al-Si-14% alloy with 1% Fe was shown to result in an ultimate tensile strength (UTS) of 174 mPa, which is 1.3 times higher than the original Z4 sample's UTS, and 2.8 times higher than Z1's. Even with a 2% Fe weight fraction in a different, Al-Si-17% sample, the addition of 0.52% Mn brought the UTS up to 161 mPa [9] p. 232. Future work could therefore involve investigating an optimal addition of manganese for these pots and whether manganese is available to the Zambian casters cheaply enough.

Further work can be done to improve the Zambian casting setup studied. Redesign of the crucible could involve safety features in addition to a change in material or lining to prevent iron dissolusion in castings. Perhaps the mold can be modified to produce a sturdier design or provide more bracing in the current design.

Acknowledgment

The authors would like to thank Ben Linder for providing the Zambian pot lids for testing, Jon Stolk and Matt Neal for their technical support in the project, and Daniel Stolk of Metallurgical Engineering Services, Inc. for optical emission spectroscopy analysis of the aluminum alloy compositions.

References

[1] Murty, B. S., S. A. Kori, and M. Chakraborty. "Grain Refinement of Aluminium and Its Alloys by Heterogeneous Nucleation and Alloying." International Materials Reviews 47.1 (2002): 3-29. Web.

[2] Hatch, John E. Aluminum: Properties and Physical Metallurgy. N.p.: ASM International, 1984. Print.

[3] Hatch, John E. Fractography. N.p.: ASM International, 1984. Volume: 12. Print.

[4] S. Dziallas, L. Little, J. McConnell, J. Perera, B. Rowley. "Zambian Pot" 2014.

[5] Mehl, Robert F. Metals Handbook. 5th ed. Vol. 7. Metals Park, Ohio: American Society for Metals, 1972. 256-60. Print.

[6] Standard Specification for Aluminum-Alloy Sand Castings, ASTM B26/B26M 05

[7] Taylor, John A. "Iron-containing Intermetallic Phases in Al-Si Based Casting Alloys." Science Direct 1 (2012): 19-33. Elsevier. Web.

[8] © 2004 Asm International. All Rights Reserved. "Introduction to Aluminum-Silicon Casting Alloys." Introduction to Aluminum-Silicon Casting Alloys (n.d.): n. pag. Asminternational.org. ASM International, 2004. Web.

[9] Belov, N. A., A. A. Aksenov, and D. G. Eskin. Iron in Aluminium Alloys: Impurity and Alloying Element. London: Taylor Francis, 2002. Print.

[10] Cao, Xinjin, and John Campbell. "Morphology of B-Al_5FeSi Phase in Al-Si Cast Alloys." Materials Transactions 47.5 (2006): 1. The Japan Institute of Metals and Materials. Web.

[11] A.L. Kearney, Properties of Cast Aluminum Alloys, Properties and Selection: Nonferrous Alloys and Special-Purpose Materials, Vol 2, ASM Handbook, ASM International, 1990